DOI: 10.1002/adem.201200048

Modeling and Simulation of Large Microstructured Particles in Magnetic-Shape-Memory Composites**

July 17, 2012

By Sergio Conti, Martin Lenz*, and Martin Rumpf

We study composite materials in which single-crystalline magnetic shape-memory particles are embedded in a polymer matrix, in the limit of particles much larger than the typical domain size. We first derive an effective macroscopic model, using the mathematical theory of relaxation, and then solve it numerically for practically relevant parameters, and compare with experimental results.

[*] *Prof. Dr. Sergio Conti,*
Institut für Angewandte Mathematik, Universität Bonn,
Endenicher Allee 60, 53115 Bonn

Dr. Martin Lenz, Prof. Dr. Martin Rumpf,
Institut für Numerische Simulation, Universität Bonn,
Endenicher Allee 60, 53115 Bonn

[**] *This work was partially supported by Deutsche Forschungsgemeinschaft through the Schwerpunktprogramm 1239* Änderung von Mikrostruktur und Form fester Werkstoffe durch äußere Magnetfelder.

1 Introduction

Magnetic shape memory (MSM) materials are characterized by two coupled phase transitions, in which a ferromagnetic order parameter (the magnetization) and a ferroelastic one (the elastic strain) interact with each other. The coupling leads to very large spontaneous strains, of the order of 10%, but also generates strong impediments to the transformation, including in particular the difficulty of forming interfaces between domains with different values of the order parameters.[1] Indeed, for each of the two order parameters low-energy interfaces are only possible with specific orientations (for example, the normal component of the magnetization should not jump across interfaces). For

this reason the transformation and the spontaneous strain are strongly suppressed in polycrystals. However, large single crystals are brittle and difficult to produce.

Magnetic shape memory (MSM) particles embedded in a polymer matrix have been proposed as a practical way of obtaining large samples with a spontaneous transformation.[2,3] Single-crystalline particles are easier to produce than large single-crystalline samples, for example by appropriately breaking up a polycrystal. Many parameters of the material, such as the size and shape of the particles, the volume fraction and the geometry of the microstructure can be at least partially controlled during the production of the composite. The elasticity constants of the matrix can be varied over several orders of magnitude (typical materials are epoxy, polyester resin and polyurethane). For the development of good composites it is important to understand the dependence of the macroscopic material properties on the microstructural parameters.

A variational model for the elastic and magnetic properties of such composites was proposed in[4] and used to study the case of composites with small MSM particles.[4,5] The model builds upon nonlinear elasticity and micromagnetism, the analysis was based on the theory of homogenization and on a numerical solution of the cell problem via the boundary-element method. The assumption of the smallness of the MSM particles leads to a crucial simplification. Small particles can be assumed to be in a single phase; in each particle the magnetization is either "up" or "down", no mixture is possible. Recent experiments used particles with size of the order of a hundred μm.[3] This is large compared to the typical size of the magnetic domains, and also compared to the typical scale of the elastic domains. Therefore we focus here on the opposite limit, in which the particles are still single crystals, but much larger than the scale of the domains.

In this paper we propose a new approach for the modeling of large MSM particles embedded in a polymer matrix, which is based on the theory of relaxation. The mathematical theory of relaxation permits to replace a complicated functional, which resolves each single domain in the microstructure, by a simpler functional, which only resolves the average material behavior of large particles and in thus better suited to numerical simulations.[6,7] The details of the microstructure are not any more explicitly resolved in the kinematics, but still correctly accounted for in the energetics; the new functional deals only with the macroscopic degrees of freedom, at a length scale much larger than the one of the microstructure.

Similar approaches have been used for a number of different physical problems, including the case of a purely magnetic phase transition and of a purely elastic phase transition. To the best of our knowledge this is the first application to a joint magnetoelastic problem. In particular, in[8] it was

shown that magnetic materials which are much larger than the characteristic length scales of the magnetic domains (the Bloch wall width, the exchange length etc.) are appropriately described by a relaxed functional in which the exchange energy does not appear, the effective magnetization may be shorter than the saturation magnetization, and the anisotropy energy is replaced by its convex envelope. Corresponding theories are much more subtle for the case of elasticity, due to the tensorial nature of the order parameter (the elastic strain). The general theory builds upon the concept of quasiconvexity, which is however very difficult to apply in practice. Indeed, up to now only in very few cases with special symmetries the relaxation was determined explicitly, see for example.[9,10] Here we build upon this general framework but approximate the quasiconvex envelope with the convex one, which is easier to compute.

The present paper is completely restricted to the two-dimensional case. Extension of the same approach to three dimensions is in principle straightforward but in practice rather cumbersome, both in the explicit computation of the convex envelope and in the numerical simulation with boundary elements. Our approach is also in many other respects only an approximation, and it is by no means clear that the restriction to two spatial dimensions is the leading error term. For the sake of simplicity we do not discuss the three-dimensional case further. It remains an open problem to compute the appropriate convex envelope in three dimensions and investigate numerically the influence of dimensionality.

We present in Section 2 the model, in Section 3 the large-particle limit, and in Section 4 we discuss our results in relation to recent experiments from.[3]

2 Micromagnetic-Elastic Model

The starting point of our analysis is the variational model from,[4] which combines elasticity and magnetism. We briefly review it here, referring to[4] for a thorough discussion of the different terms.

We work here with geometrically linear elasticity in two dimensions. We denote by $\Omega \subset \mathbb{R}^2$ the domain occupied by the composite, and by $\omega \subset \Omega$ the part which is occupied by the particles, $\omega = \cup_i \omega_i$.

The elasticity is described through the elastic displacement field $u : \Omega \to \mathbb{R}^2$, magnetism through the magnetization $M : \mathbb{R}^2 \to \mathbb{R}^2$ (we set $M = 0$ outside the volume occupied by the particles, i.e., both in the polymer and in vacuum). The position of the material point x in the deformed configuration is then given by the deformation field $v(x) = x + u(x)$, which we assume to be injective

on Ω. Additionally we introduce a phase variable, $p : \omega \to \{0, 1\}$, which characterizes the two phases of the material. The variables u, v and p are defined on the reference configuration, whereas M is defined on the deformed configuration.

The elastic energy is written separately in the MSM particles and in the polymer and takes the form

$$E_{\text{elast}} = \int_{\omega} W_{\text{MSM}}((\nabla u(x))Q(x) - \varepsilon_{p(x)})\, dx + \int_{\Omega\setminus\omega} W_{\text{pol}}(\nabla u(x))\, dx\,, \tag{1}$$

where $Q : \omega \to SO(2)$ represents the crystal lattice orientation in the reference configuration (constant in each particle) and ε_p is the spontaneous strain in phase p,

$$\varepsilon_0 = \begin{pmatrix} -\overline{\varepsilon} & 0 \\ 0 & \overline{\varepsilon} \end{pmatrix}, \qquad \varepsilon_1 = \begin{pmatrix} \overline{\varepsilon} & 0 \\ 0 & -\overline{\varepsilon} \end{pmatrix}. \tag{2}$$

The energy density W_{MSM} penalizes deviations of the strain from ε_p, and is here parametrized with the cubic elastic constants C_{11}, C_{12} and C_{44}. The polymer matrix is assumed to be an isotropic, linearly elastic material and its energy density W_{pol} is parametrized by the elastic modulus E and Poisson's ratio ν.

The magnetic energy depends on the magnetization field $M : \mathbb{R}^2 \to \mathbb{R}^2$, which has length $|M| = M_s$ on the deformed particles, i.e., on $v(\omega)$, and vanishes elsewhere. Here M_s denotes the saturation magnetization. As usual in micromagnetism we include a coupling to the external field H_{ext}, the demagnetization term, and the phase-dependent anisotropy term:

$$E_{\text{mag}} = \int_{\mathbb{R}^2} \frac{1}{2}\frac{1}{\mu_0}|H_d|^2 - \frac{1}{\mu_0} H_{\text{ext}} \cdot M\, dy + K_u \int_{v(\omega)} \varphi_{p(v^{-1}(y))} \left((Q(v^{-1}(y)))^T M\right)\, dy\,. \tag{3}$$

Notice that we neglect the exchange term $\int |DM|^2 dy$, this is appropriate for the case of particles much larger than the domains we are interested in. The field $H_d : \mathbb{R}^2 \to \mathbb{R}^2$ is the projection of M onto curl-free fields, i.e., it solves $\text{div} H_d = \text{div} M$ and $\text{curl} H_d = 0$. The distinction between the two phases enters via the anisotropy, which in the model takes the form $\varphi_0(M) = \frac{M_2^2}{|M|^2}\,, \varphi_1(M) = \frac{M_1^2}{|M|^2}$. Further, K_u is the uniaxial anisotropy constant, and working in a linearized setting we ignore the rotation associated with the elastic deformation v inside the anisotropy term.

We use parameters for NiMnGa, precisely: $\frac{M_s}{\mu_0} \simeq 0.50 \frac{\text{M Pa}}{\text{T}}$,[11] $K_u \simeq 0.13$ M Pa,[12] $\overline{\varepsilon} \sim 0.058$, $C_{11} = 160$ G Pa, $C_{44} = 40$ G Pa, $C_{11} - C_{12} = 4$ G Pa.[13] For the polymer we fix $\nu = 0.4$ and vary E.

3 Large-Particle Model

The particles used in the experiments are much larger than the typical domain size.[3] Numerically resolving each domain becomes very difficult, but a substantial simplification of the model can be achieved by an analytical treatment of the domain structure.[8] In particular, we assume that in each particle a fine mixture of different domains may appear, on a scale which is much smaller than the size of the particles. Our aim is to characterize the behavior of the entire particle in terms of average variables, namely, the average magnetization in the particle and a continuous phase variable describing the volume fraction of the two phases.

Consider a particle ω_i which is entirely in one phase, say $p = 1$. The magnetization is a vector field $M : v(\omega_i) \to \mathbb{R}^2$, with constant length M_s. If M oscillates on a very fine scale between two values, say $(M_s, 0)$ and $(0, M_s)$, and each of them is taken on half of the volume of the particle, the average magnetization will be $\frac{1}{2}(M_s, 0) + \frac{1}{2}(0, M_s) = (\frac{M_s}{2}, \frac{M_s}{2})$, a vector whose length $M_s/\sqrt{2} \sim 0.71 M_s$ is less than M_s. By similar constructions all vectors with length less than or equal to M_s can be generated as average magnetization of the particle. Mathematically, this transforms the non-convex constraint $|M| = M_s$ for the magnetization M into the convex constraint $|M| \leq M_s$. The macroscopic analysis will then focus on the average magnetization, which obeys the convex constraint, and ignore the fine-scale oscillations. If the energy is replaced by the appropriate macroscopic effective energy this leads to a substantial simplification of the variational problem without major changes in the predictions, see.[6,7,14] Similar ideas have been exploited successfully to study magnetization patterns in magnetic thin films, for example in,[15] and elastic microstructures in liquid crystal elastomers, for example in.[10] Here the situation is however more complex, since we have both a magnetization and a phase parameter which couples to the elastic degrees of freedom. In both the purely magnetic and the purely elastic example, a proper mathematical treatment shows that continuity of the deformation at the interface and the energetic cost of a nonzero divergence of the magnetization lead to constraints on the geometry of the possible microstructure, which influence the precise form of the effective energy.[10,15] For the sake of simplicity we ignore here these effects and use the convex envelope instead of the quasiconvex envelope of the energy density (see[6,7] for precise definitions). This is clearly only an approximation, we shall however see that it suffices to obtain qualitatively correct results.

We rewrite the anisotropy energy φ entering the last term in (3) as a function γ of the phase

parameter $p \in \{0,1\}$ and the scaled magnetization $m = M/M_s$,

$$\gamma(p,m) = \begin{cases} m_2^2 & \text{for } p = 0 \text{ and } |m| = 1\,, \\ m_1^2 & \text{for } p = 1 \text{ and } |m| = 1\,. \end{cases} \tag{4}$$

Optimizing over all possible microstructures which generate a given average phase $p \in [0,1]$ and magnetization m, $|m| \leq 1$, corresponds to replacing γ by its convex envelope γ^{conv}, which is the largest convex function which is nowhere larger than γ.

We start from the case $p = 0$. Consider an average magnetization m with $|m| \leq 1$. Then there are two admissible microscopic magnetizations m^+, m^- which have weighted average m and the same second component as m. Equivalently, m^+ and m^- are two vectors which obey $|m^+| = |m^-| = 1$, $m = \lambda m^+ + (1-\lambda)m^-$ for some $\lambda \in [0,1]$ and $m_2 = m_2^+ = m_2^-$; one can see that the pair $m^\pm = (\pm\sqrt{1-m_2^2}, m_2)$ with $\lambda = (m_1 + \sqrt{1-m_2^2})/(2\sqrt{1-m_2^2})$ will do. If the magnetization oscillates on a fine scale between the two values m^+ and m^-, one achieves the required average magnetization m with average energy density given by $\gamma(0,m^+) = \gamma(0,m^-) = m_2^2$ (see **Figure 1(a)** for an illustration). The convexity of this expression shows that the microstructure constructed is optimal, in the sense that no other admissible construction has lower average energy. Therefore we conclude that $\gamma^{\text{conv}}(0,m) = m_2^2$. Analogously, one sees that $\gamma^{\text{conv}}(1,m) = m_1^2$.

We pass now to the situation in which the two phases are mixed. Consider a pair (p,m), with $|m| \leq 1$ and $0 < p < 1$. A volume fraction p of the particle will be in phase 1, we denote by a the average magnetization of this part. Analogously, b denotes the average magnetization of the rest, which is in phase 0 and corresponds to a volume fraction $1-p$. Since the average magnetization equals m, and a, b must be achievable as average magnetizations, necessarily

$$pa + (1-p)b = m\,, \quad |a| \leq 1\,, \quad |b| \leq 1\,. \tag{5}$$

The precise choice of a and b will be dictated by minimization of the average energy, which takes the form

$$p\gamma(0,a) + (1-p)\gamma(1,b) = pa_1^2 + (1-p)b_2^2\,. \tag{6}$$

Practically, one seeks of a and b subject to the constraints (5) which minimize (6). This can be done by the standard method of Lagrange multipliers, leading to a somewhat cumbersome but straightforward computation (cf. Appendix). In order to illustrate the result, we discuss the different regimes which

play a role in the minimization (see **Figure 1(b)** for an illustration).

Case I: For some values of (p, m) one can achieve zero energy. This occurs when there are admissible choices of a and b with $a_1 = b_2 = 0$. Hence we need to take $pa_2 = m_2$ and $(1-p)b_1 = m_1$; this choice is admissible for all (p, m) such that $|m_1| \leq 1 - p$ and $|m_2| \leq p$. This set is the tetrahedron with vertices $(0, 0, 1)$, $(0, 0, -1)$, $(1, 1, 0)$, $(1, -1, 0)$.

Case II: If (p, m) is outside the tetrahedron, but $|m_1| \leq \sqrt{(1 - |m_2|)(1 + |m_2| - 2p)}$, then the optimal choice is $a = (0, \pm 1)$ (depending on the sign of m_2) and $b = (b_1, (m_2 \mp p)/(1-p))$ for some b_1; the resulting energy is $(1-p)b_2^2 = (m_2 \mp p)^2/(1-p) = (|m_2| - p)^2/(1-p)$. The condition for $|m_1|$ follows from the constraint $|b| \leq 1$. Analogously there is a regime in which $b = (\pm 1, 0)$ and $a_1 \neq 0$. This corresponds to one of the two terms in (6) vanishing.

Case III: both terms in (6) contribute to the energy, and $|a| = |b| = 1$. Solving $pa + (1-p)b = m$ for a or b, respectively, and inserting this into $|a| = |b| = 1$ yields

$$m \cdot a = \frac{|m|^2 + p^2 - (1-p)^2}{2p}, \qquad m \cdot b = \frac{|m|^2 + (1-p)^2 - p^2}{2(1-p)}.$$

From these one can compute the angles between m and a or b, respectively, and get

$$\begin{aligned} \gamma_{\mathrm{III}}(p, m) =& p \sin^2 \left(\sin^{-1} \frac{|m_1|}{|m|} - \cos^{-1} \frac{|m|^2 - 1 + 2p}{2p|m|} \right) \\ &+ (1-p) \cos^2 \left(\cos^{-1} \frac{|m_2|}{|m|} + \cos^{-1} \frac{|m|^2 + 1 - 2p}{2(1-p)|m|} \right). \end{aligned} \tag{7}$$

The final result is

$$\gamma^{\mathrm{conv}}(p, m) = \begin{cases} 0 & \text{if } |m_1| \leq 1 - p \text{ and } |m_2| \leq p\,, \\ \dfrac{(|m_2| - p)^2}{1-p} & \text{if } |m_1| \leq \sqrt{(1 - |m_2|)(1 + |m_2| - 2p)}\,, \\ \dfrac{(|m_1| - 1 + p)^2}{p} & \text{if } |m_2| \leq \sqrt{(1 - |m_1|)(2p + |m_1| - 1)}\,, \\ \gamma_{\mathrm{III}}(p, m) & \text{otherwise.} \end{cases}$$

Therefore in the large-particle limit the magnetic energy (3) is approximated by

$$E_{\mathrm{mag}}^{\mathrm{relax}} = \int_{\mathbb{R}^2} \frac{1}{2} \frac{1}{\mu_0} |H_d|^2 - \frac{1}{\mu_0} H_{\mathrm{ext}} \cdot M \, dy + K_u \int_{v(\omega)} \gamma^{\mathrm{conv}}(p(v^{-1}(y)), \left((Q(v^{-1}(y)))^T M \right) \, dy \tag{8}$$

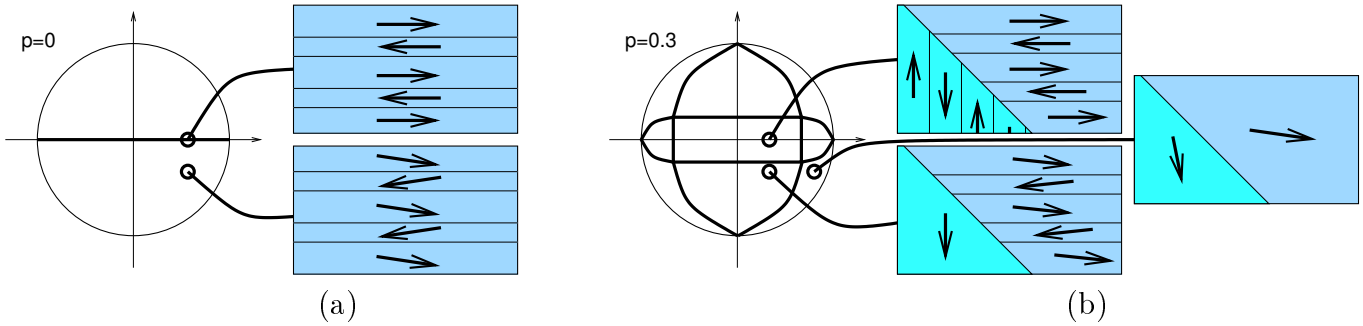

Figure 1: Sketch of the microstructures used in the relaxation of the anisotropy energy. Left panel: construction for $p = 0$. One keeps the m_2 component constant, and lets the m_1 component oscillate in order to generate the appropriate average. Right panel: Construction for the intermediate value $p = 0.3$, illustrating the three cases discussed in the text.

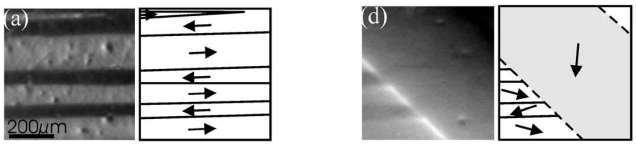

Figure 2: Magnetic domain patterns for different applied fields perpendicular to the easy axis. The sketches represent the direction of the magnetization in the different domains, to be compared with the patterns used in the relaxation illustrated in Figure 1. Reprinted with permission from.[16] Copyright 2007, American Institute of Physics.

and the eigenstrains (2) entering the elastic energy are replaced by the appropriate weighted average,

$$\varepsilon_p = (1-p)\varepsilon_0 + p\varepsilon_1 = \begin{pmatrix} (2p-1)\overline{\varepsilon} & 0 \\ 0 & (1-2p)\overline{\varepsilon} \end{pmatrix} . \tag{9}$$

As noted above, replacing the anisotropy energy by its convex envelope is an underestimate of the true energy, since the additional stray field and the additional elastic tensions generated by the "inner" interfaces are neglected. As discussed above, a finer analysis is beyond the scope of this work.

4 Results on the macroscopic behavior of composites

In order to obtain quantitative predictions on the properties of the composite material from our model one also needs to account for the second level of structure present on a mesoscale in the sample, which is given by the geometry of the particle-polymer mixture and describes the interaction between the MSM particles and the matrix. As in the case of small particles[4] we work within the theory of homogenization[14] assuming that the microstructure is periodic and that each periodic cell contains a small number of particles. We use boundary elements[17] to express both the elastic and the magnetic problem in the full space in terms of the deformation and the magnetization on the

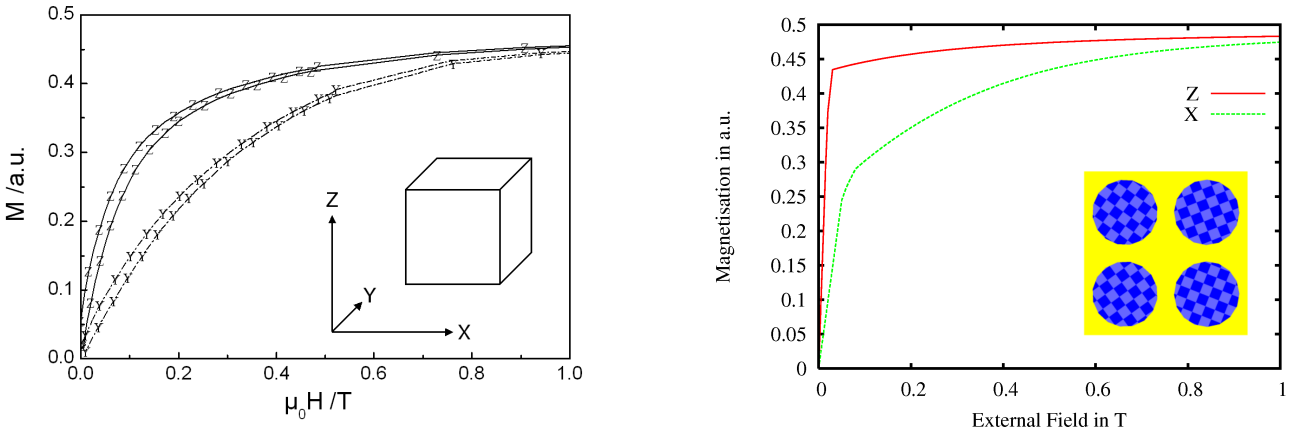

(a) (b)

Figure 3: Left panel: experimental measurements of the total magnetization as a function of applied magnetic field with two different orientations, reprinted from,[3] copyright 2007, with permission from Elsevier. Right panel: corresponding simulation.

boundary of each particle, and a gradient descent approach to minimize the energy. Details are given in.[4]

In order to validate our approach we compare our simulation results in **Figure 3** with experimental measurements from.[3] In the experiments a partial orientation of the particles had been obtained via a careful curing process under an applied magnetic field in the Z direction, we simulate that by imposing minor variations of the crystal orientation Q among the four particles included in the unit cell. For a specific geometry of the composite, which has been chosen to match qualitatively the samples used in the experiments, we compute the total magnetization for different values of the external field, in two different orientations (which are not equivalent due to the mentioned orientational ordering). The volume fraction of MSM particles is approximately 1/4. The qualitative behavior with a gradual switching is in good agreement with experiment, and also the amount of magnetic field needed to reach saturation is reproduced well.

As a next step, we use the current model to guide future experiments and to understand the dependence of the macroscopic behavior of the composite on the parameter describing the microstructure. The key variables which are experimentally accessible are the volume fraction of MSM particles, the type of polymer and the amount of alignment obtained during curing. We work with the same four round grains in the unit cell as in **Figure 3**, parametrize the polymers by Young's elastic modulus, and the alignment by the average orientational difference of the four grains from the magnetization direction. One parameter of interest is the total macroscopic strain which is achieved under transformation, this is illustrated in **Figure 4**. Clearly the strain is maximal when the polymer is very soft, because the transformation of the grains is not hindered. However, the very softness of the

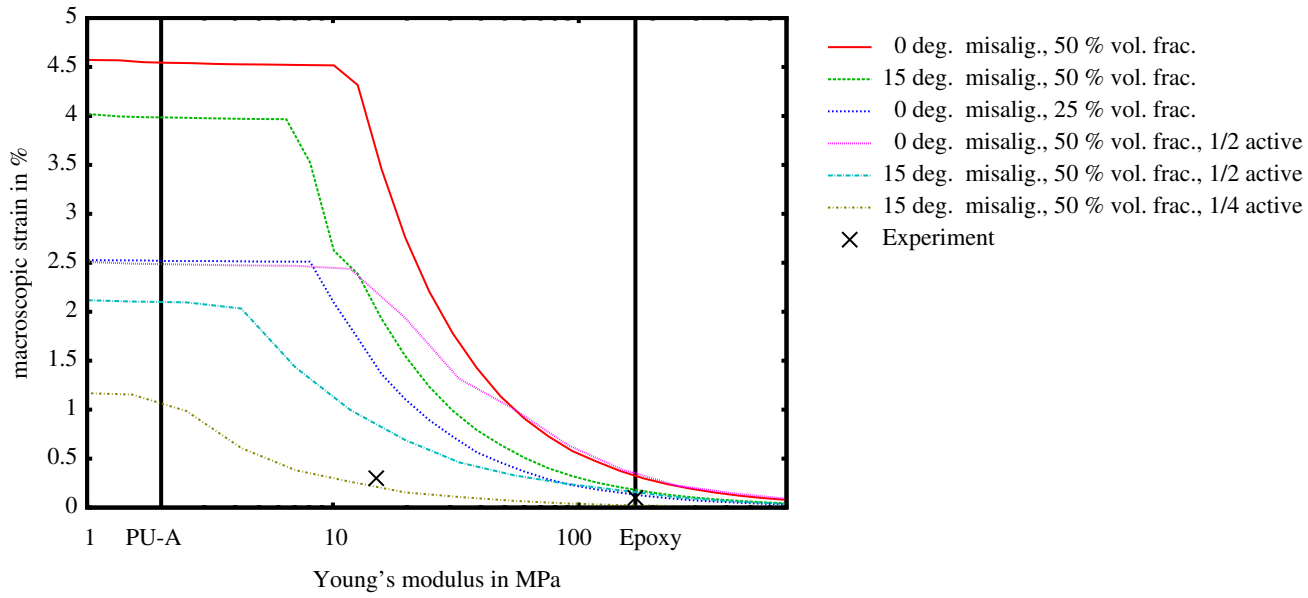

Figure 4: Expected macroscopic strain as a function of Young's modulus of the polymer matrix for different microstructures. The geometry of the sample is the same as in Figure 3. The different curves correspond to different volume fractions of MSM material and different misalignment angles. Additionally, three curves in which only some of the MSM particles are active are included.

polymer makes the transmitted force very small, and in the limit of very soft polymers the material is unusable. Therefore we focus on the work output, which measures the amount of energy stored in the material when it is not permitted to elongate, and therefore characterizes the amount of work that the material can perform when used as an actuator. **Figure 5** shows that Young's moduli of the polymer of the order of 1 to 10 MPa deliver the optimal work output, depending on the other microstructural parameters. This is close to the value of the matrix used in,[3] and substantially smaller than the elastic modulus of the previously used Epoxy.

5 Concluding remarks

We presented a model for studying MSM-polymer composites with particles which are much larger than the domain size, in two spatial dimensions. The subgrain microstructure is treated by replacing the spontaneous strain and the anisotropy by their convex envelopes; this has the advantage of delivering explicit formulas but comes at the cost of ignoring the additional magnetic and elastic energy coming from incompatibility at the interfaces. We used the model to simulate numerically the behavior of specific composites, obtained good agreement with experimental results and provided indications on the influence that various microstructural parameters have on the macroscopic material properties, in particular on the spontaneous strain and the work output. Interesting pos-

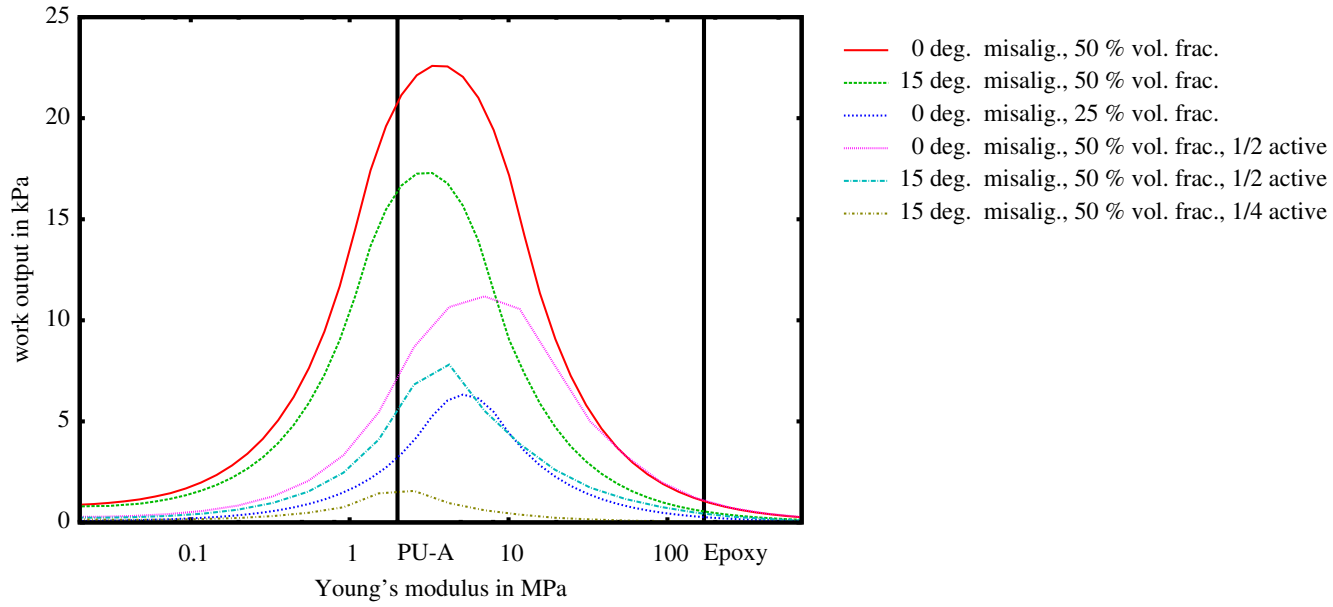

Figure 5: Expected work output as functions of Young's modulus of the polymer matrix for different microstructures (same samples as in Figure 4).

sible developments include the treatment of incompatibilities at the interfaces and the extension to a time-dependent setting, for example via a model which includes rate-independent motion of the interfaces.

References

[1] a) K. Ullakko, J. K. Huang, C. Kantner, R. C. O'Handley, V. V. Kokorin, *Appl. Phys. Lett.* **1996**, *69*, 1966; b) A. Sozinov, A. A. Likhachev, N. Lanska, K. Ullako, *Appl. Phys. Lett.* **2002**, *80*, 1746.

[2] J. Feuchtwanger *et al.*, *J. Appl. Phys.* **2003**, *93*, 8528.

[3] N. Scheerbaum, D. Hinz, O. Gutfleisch, K.-H. Müller, L. Schultz, *Acta Mater.* **2007**, *55*, 2707.

[4] S. Conti, M. Lenz, M. Rumpf, *J. Mech. Phys. Solids* **2007**, *55*, 1462.

[5] S. Conti, M. Lenz, M. Rumpf, *Mat. Sci. Engrg. A* **2008**, *481-482*, 351.

[6] B. Dacorogna, *Direct methods in the calculus of variations*, Springer-Verlag, New York, **1989**.

[7] S. Müller in *Variational models for microstructure and phase transitions* (Eds.: F. Bethuel *et al.*), Springer, Berlin, **1999**, p. 85.

[8] a) A. Desimone, *Arch. Rat. Mech. Anal.* **1993**, *125*, 99; b) R. D. James, D. Kinderlehrer, *Continuum Mechanics and Thermodynamics* **1990**, *2*, 215.

[9] A. DeSimone, G. Dolzmann, *Arch. Rat. Mech. Anal.* **2002**, *161*, 181.

[10] S. Conti, A. DeSimone, G. Dolzmann, *J. Mech. Phys. Solids* **2002**, *50*, 1431.

[11] A. A. Likhachev, K. Ullakko, *Phys. Lett.* **2000**, *A 275*, 142.

[12] O Söderberg, Y. Ge, A. Sozinov, S.-P. Hannula, V. K. Lindroos, *Smart Mater. Struct.* **2005**, *14*, 223.

[13] M. Stipcich *et al.*, *Phys. Rev. B* **2004**, *70*, 054115.

[14] A. Braides, A. Defranceschi, *Homogenization of multiple integrals*, Claredon Press, Oxford, **1998**.

[15] A. DeSimone, R. Kohn, S. Müller, F. Otto, R. Schäfer, *J. Magn. Magn. Mat.* **2002**, *242-245*, 1047.

[16] Y. W. Lai, N. Scheerbaum, D. Hinz, O. Gutfleisch, R. Schäfer, L. Schultz, J. McCord, *Appl. Phys. Lett.* **2007**, *90*, 192504.

[17] W. Hackbusch, *Integral equations – Theory and numerical treatment*, Birkhäuser Verlag, **1995**.

6 Appendix

In order to carry out the minimization of (6) under the constraints (5) we set $d = a - b$, which together with the first constraint allows to write $a = m + (1-p)d$ and $b = m - pd$. Inserting a and b into the energy (6) the remaining degrees of freedom are just d_1 and d_2, and the constraints are $|a|, |b| \leq 1$.

To derive necessary conditions, we formulate the Lagrange function in terms of d_1, d_2 with Lagrange

multipliers λ_1, λ_2 for the two constraints

$$\begin{aligned}
L(d_1,d_2,\lambda_1,\lambda_2) :=& f(d_1,d_2)+\lambda_1 g_1(d_1,d_2)+\lambda_2 g_2(d_1,d_2), \text{ where}\\
f(d_1,d_2) :=& p\big(m_1+(1-p)d_1\big)^2+(1-p)\big(m_2-pd_2\big)^2,\\
g_1(d_1,d_2) :=& \big(m_1+(1-p)d_1\big)^2+\big(m_2+(1-p)d_2\big)^2-1,\\
g_2(d_1,d_2) :=& \big(m_1-pd_1\big)^2+\big(m_2-pd_2\big)^2-1,
\end{aligned}$$

and compute the Karush–Kuhn–Tucker conditions

$$\frac{\partial}{\partial d_1}L(d_1,d_2,\lambda_1,\lambda_2)=0, \qquad \frac{\partial}{\partial d_2}L(d_1,d_2,\lambda_1,\lambda_2)=0, \tag{10}$$

$$\lambda_1 g_1(d_1,d_2)=0, \qquad \lambda_2 g_2(d_1,d_2)=0, \tag{11}$$

$$\lambda_1 \geq 0, \qquad \lambda_2 \geq 0, \tag{12}$$

$$g_1(d_1,d_2)\leq 0, \qquad g_2(d_1,d_2)\leq 0. \tag{13}$$

We first compute (10):

$$2p(1-p)(m_1+(1-p)d_1)+2\lambda_1(1-p)(m_1+(1-p)d_1)-2\lambda_2 p(m_1-pd_1)=0 \tag{14}$$

$$-2p(1-p)(m_2-pd_2)+2\lambda_1(1-p)(m_2+(1-p)d_2)-2\lambda_2 p(m_2-pd_2)=0 \tag{15}$$

Condition (11) allows to distinguish four cases:

a) $\lambda_1=\lambda_2=0$. Then (14),(15) give $m_1+(1-p)d_1=m_2-pd_2=0$, or equivalently $a_1=b_2=0$. Thus we are in case I discussed above.

b) $\lambda_1>0$, $\lambda_2=0$. On the one hand, $g_1(d_1,d_2)=0$, which means $|a|=1$. On the other hand, from (14) one derives $2(1-p)(p+\lambda_1)(m_1+(1-p)d_1)=0$, which means $m_1+(1-p)d_1=a_1=0$ (case II). The case $\lambda_1=0$, $\lambda_2>0$ behaves analogously.

c) $\lambda_1>0$ and $\lambda_2>0$. Thus, $g_1(d_1,d_2)=g_2(d_1,d_2)=0$. This means $|a|=|b|=1$, which is case III.